Bio-Medical Materials and Engineering 24 (2014) 2751–2760
DOI 10.3233/BME-141093
IOS Press

Automatic recognition of facial movement for paralyzed face

Ting Wang, Junyu Dong*, Xin Sun, Shu Zhang and Shengke Wang
Department of Computer Science and Technology, Ocean University of China, Songling Road 268th, Qingdao 266100, China

Abstract. Facial nerve paralysis is a common disease due to nerve damage. Most approaches for evaluating the degree of facial paralysis rely on a set of different facial movements as commanded by doctors. Therefore, automatic recognition of the patterns of facial movement is fundamental to the evaluation of the degree of facial paralysis. In this paper, a novel method named Active Shape Models plus Local Binary Patterns (ASMLBP) is presented for recognizing facial movement patterns. Firstly, the Active Shape Models (ASMs) are used in the method to locate facial key points. According to these points, the face is divided into eight local regions. Then the descriptors of these regions are extracted by using Local Binary Patterns (LBP) to recognize the patterns of facial movement. The proposed ASMLBP method is tested on both the collected facial paralysis database with 57 patients and another publicly available database named the Japanese Female Facial Expression (JAFFE). Experimental results demonstrate that the proposed method is efficient for both paralyzed and normal faces.

Keywords: Facial paralysis, facial movement, active shape models, local binary patterns

1. Introduction

Facial paralysis is a common disease whose prominent feature is dysfunction of facial muscle movement. It occurs on either side of the face which makes patients' faces asymmetric. Besides its effects on physical health, facial disfigurement may have an adverse impact on the patient's psychology. To evaluate the degree of facial paralysis, the internist firstly asks the patient to perform a set of facial movements related to different regions of the face, and then assesses the degree of facial paralysis based on the facial movement patterns. One of the fundamental issues for automatic diagnosis of facial paralysis is to identify the facial movement patterns accurately.

Several grading quantification methods for the evaluation of facial paralysis have been developed. Most of these methods are based on the following hypothesis: the measurement is conducted under the prior knowledge of the facial movement patterns [1–6], while a few methods also conduct measurement based on different facial motion patterns stored under pre-defined sequence with the rest face between each pattern for motion discrimination [7–9]. All of these methods require the doctor to confirm that each facial action is performed completely and the rest face is also performed between

*Corresponding author: Junyu Dong, Department of Computer Science and Technology, Ocean University of China, Songling Road 268th, Qingdao 266100, China. Tel.: +86-532-66782300; Fax: +86-532-66782300; E-mail: dongjunyu@ouc.edu.cn.

each facial movement. Moreover, remote diagnosis of facial paralysis is gaining larger popularity due to the fast development of computer network and multimedia technology. There are desperate needs for completely automatic facial paralysis evaluation system without human intervention. As a fundamental step, automatic recognition of facial movement patterns is important. To date, plenty of feature extraction methods have been proposed to extract holistic [10,11] or local [12,13] features to recognize the facial expression from normal human's faces. Meanwhile, Action Units (AUs) [14,15] or dense optical flow [16,17] based methods are also introduced to recognize the facial expression. However, all of these methods require human participation or have subjective threshold dependence. Furthermore, these methods show good performance in the recognition of facial expression on the normal human faces, but poor performance on the abnormal human faces.

This paper presents an automatic, objective, and effective method to recognize the facial movement patterns of facially paralyzed patients. The proposed method firstly locates the positions of 68 facial key points using Active Shape Models (ASMs) [18] on each of human faces. Then, it normalizes these faces based on the positions of pupils and the apex of nose. Thirdly, it extracts Local Binary Patterns (LBP) [19] features from eight facial regions. In order to increase the robustness and flexibility, the positions of eight local facial regions are located based on the facial key points detected by ASMs. Finally, experiments are carried out by Support Vector Machine (SVM) to evaluate the performance of the proposed method on the collected facial paralysis database and the Japanese Female Facial Expression (JAFFE) database [20] respectively. The contributions of this paper include: (a) patients do not have to perform several facial movements in a fixed order as required in [7–9]; (b) different facial movement patterns of a paralyzed face can be recognized automatically; (c) the method can not only be used for diagnosis of facial paralysis but also for recognizing exaggerated expression or grimace of a normal person.

2. Materials and methods

2.1. Data collection

A database containing a number of paralyzed faces has been constructed from September, 2012 to September, 2013 in the hospital of Hiser Medical Center, Qingdao. This database contains 57 patients of facial paralysis including 31 females and 26 males. The age of patients ranges from seven to sixty-eight years old.

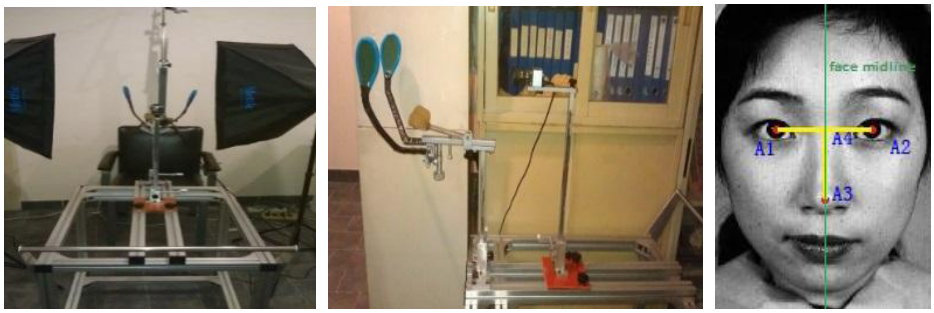

(a) (b) (c)

Fig. 1. (a) and (b) The equipment and environment for collecting patients' facial images from different viewpoints. (c) The demonstration of facial image normalization (This facial image is from the JAFFE database).

The equipment and environment for image collection are shown in the Figures 1(a) and 1(b). Patients have to perform five basic facial movements, i.e., raising eyebrows, closing eyes, screwing up nose, plumping cheek and opening mouth, which have been used as a standard clinically.

2.2. Preprocessing of facial images

There are very few constraints for collecting patients' facial samples in the hospital, such as illuminations, which gives doctors more freedom for collecting the samples. However, patients usually choose a comfortable sitting posture which may lead to a slight angle variance of face orientation. Meanwhile, it is difficult to keep the distance between patient and camera consistent. In order to solve the above problems and increase the robustness of the proposed method, the raw images are preprocessed through the following steps.

Firstly, ASMs are used to fit the face of a patient so as to locate the positions of pupils (A1, A2) and the position of the apex of nose (A3), as shown in Figure 1(c). The midline of face is defined as the line across the midpoint A4 of (A1, A2) and the apex nasi A3.

Secondly, the face images should be normalized according to [21] with some modifications as follows: The length of $\overline{P_{A1}P_{A2}}$ is scaled to 68 pixels, and the length between point A1 and the top of the image in the vertical direction is scaled to 85 pixels. The goal of normalization is to establish a common coordinate system so that different faces can be easily compared. Each image is then cropped into a 138×196 rectangle image. Thus, all normalized faces have the same scale: the vertical coordinate of point A1 is 85($A1_y$=85) and $\overline{P_{A1}P_{A2}}$=68 (Upper-left corner has the coordinate of [0, 0]).

2.3. Location of the facial key regions

There are a number of model-based algorithms that can be used to detect the facial features, such as deformable geometric templates [22] and active contour models [23]. However, the fitting results of these algorithms may converge to incorrect local minima because of the inaccurate initializations and large facial feature variances. The Deformable Part Model (DPM), which was introduced by Felzenszwalb et al. [24], has shown remarkably good results for category-level object detection. Nevertheless, DPM is difficult to accurately detect small local regions of the face. The ASMs, proposed by Cootes and Taylor [18], can adapt to any predefined shapes more accurately and effectively. Thus, it has been successfully used to extract the facial features of a face image under frontal view [25].

In the proposed method, the ASMs are introduced to locate 68 points on the face of a facially paralyzed patient. The positions of 68 key points are shown in Figure 2(a). In order to make the positions of key points as accurate as possible, firstly the facial paralysis images with 68 landmarks annotated on each are used to train the ASMs. Then, the trained model is used to fit the face from a new patient. The fitting result is shown in Figure 2(b).

After these 68 points are positioned, the face is divided into eight regions, as shown in Figure 2(c). The face areas are segmented by two steps. Firstly, it defines the width (noted as w_i) and height (noted as h_i) of eight facial rectangle regions, $i \in$ {Eyebrow, Left-Eye, Right-Eye, Upper-Nose, Low-Nose, Left-Cheek, Right-Cheek, Mouth}, based on the longest width and the highest height of their corresponding regions respectively in all the training data. Considering that different movements can make changes on the shapes and positions of facial organs, the proposed method uses $1.2\times w_i$ and $1.2\times h_i$ as the width and height for Eyebrow, Eye and Nose regions respectively, $1.0\times w_i$ and $1.2\times h_i$ for Cheek regions, and $1.2\times w_i$ and $3.0\times h_i$ for Mouth region. Secondly, it defines the locations of each

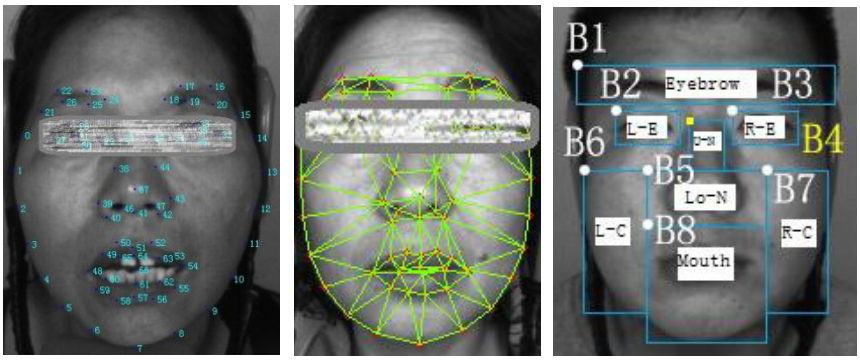

(a) (b) (c)

Fig. 2. (a) The positions of 68 key points on the face. (b) The fitting result of 68 points by using ASMs. (c) Diagram of facial regions.
Note: Eyebrow: Eyebrow region, E: Eye region, N: Nose region, C: Cheek region, Mouth: mouth region, L: Left, R: Right, U: Upper, Lo: Lower.

region based on the rule that the facial organ should be in the center of the rectangle region with a dynamic displacement (α_n along the x-axis and β_n along the y-axis). The dynamic displacements are calculated from the positions of the key points of the organ. The details of locating the eight regions are shown as follows:

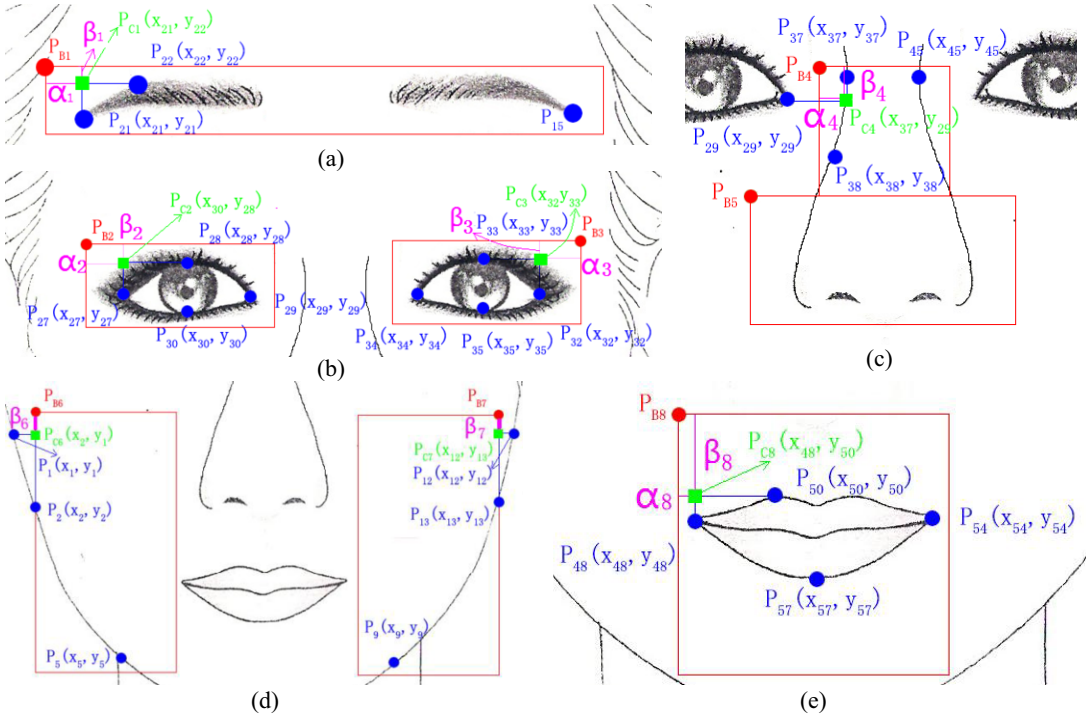

Fig. 3. Illustration of the points and parameters which are used to locate the eight rectangle regions.

1. The Eyebrow rectangle region is defined with a width of $1.2\times w_{Eyebrow}$=120 pixels, and a height of $1.2\times h_{Eyebrow}$=18 pixels as shown in Figure 2(c). The upper-left corner is point B1. As illustrated in Figure 3(a), the position of point B1 is determined by the following steps: (a) Point C1 is the intersection of the horizontal line through point 22 and the vertical line through point 21; (b) The distance $\overline{P_{15}P_{21}}$ between point 15 and point 21 along the x-axis and the distance $\overline{P_{21}P_{22}}$ between point 22 and point 21 along the y-axis are calculated; (c) Let α_1=$0.5\times|\overline{P_{15}P_{21}}-1.2\times w_{Eyebrow}|$, and β_1=$0.5\times|\overline{P_{21}P_{22}}-1.2\times h_{Eyebrow}|$; (d) The upper-left corner Point B1 ($x_{P_{B1}}$,$y_{P_{B1}}$) can be located based on Eq. (1).

$$x_{\mathrm{P_{B1}}} = x_{\mathrm{P_{21}}} - \alpha_1,\ y_{\mathrm{P_{B1}}} = y_{\mathrm{P_{22}}} - \beta_1 \tag{1}$$

2. Similar to the region of Eyebrow, the Left-Eye rectangle region is obtained with $1.2\times w_{Lfet\text{-}Eye}$=36 pixels width and $1.2\times h_{Left\text{-}Eye}$=18 pixels height, and its upper-left corner is point B2, as shown in Figure 2(c). The position of B2 is determined by the following steps: (a) Point C2 is the intersection of the horizontal line through point 28 and the vertical line through point 27; (b) $\overline{P_{27}P_{29}}$ between point 27 and point 29 along the x-axis and $\overline{P_{28}P_{30}}$ between point 28 and point 30 along the y-axis are calculated; (c) Let α_2 =$0.5\times|\overline{P_{27}P_{29}}-1.2\times w_{Lfet\text{-}Eye}|$, and β_2 =$0.5\times|\overline{P_{28}P_{30}}-1.2\times h_{Left\text{-}Eye}|$; (d) The upper-left corner Point B2 ($x_{P_{B2}}$,$y_{P_{B2}}$) is then located based on the Eq. (2). Similarly, the position of B3 can be calculated by Eq. (3) for the Right-Eye rectangle region. And let $w_{Right\text{-}Eye}$=$w_{Left\text{-}Eye}$, $h_{Right\text{-}Eye}$=$h_{Left\text{-}Eye}$,α_3=$0.5\times|\overline{P_{32}P_{34}}-1.2\times w_{Right\text{-}Eye}|$, and β_3=$0.5\times|\overline{P_{33}P_{35}}-1.2\times h_{Right\text{-}Eye}|$. The process for defining Eyes regions is illustrated in Figure 3(b).

$$x_{\mathrm{P_{B2}}} = x_{\mathrm{P_{27}}} - \alpha_2,\ y_{\mathrm{P_{B2}}} = y_{\mathrm{P_{28}}} - \beta_2 \tag{2}$$

$$x_{\mathrm{P_{B3}}} = x_{\mathrm{P_{32}}} + \alpha_3,\ y_{\mathrm{P_{B3}}} = y_{\mathrm{P_{33}}} - \beta_3 \tag{3}$$

3. The Upper-Nose region can be defined as a rectangle with $1.2\times w_{Upper\text{-}Nose}$=24 pixels width, $1.2\times h_{Upper\text{-}Nose}$=30 pixels height. Its upper-left corner is point B4, as shown in Figure 2(c). The position of point B4 is determined according to the following steps: (a) Point C4 is the intersection of the horizontal line through point 29 and the vertical line through point 37; (b) $\overline{P_{37}P_{45}}$ between point 37 and point 45 along the x-axis and $\overline{P_{29}P_{38}}$ between point 29 and point 38 along the y-axis are calculated; (c) Let α_4=$0.5\times|\overline{P_{37}P_{45}}-1.2\times w_{Upper\text{-}Nose}|$, and β_4=$0.5\times|\overline{P_{29}P_{38}}-1.2\times h_{Upper\text{-}Nose}|$; (d) The upper-left corner Point B4 ($x_{P_{B4}}$,$y_{P_{B4}}$) is then located based on the Eq. (4). Meanwhile, the Low-Nose rectangle region is defined as $1.2\times w_{Lower\text{-}Nose}$=54 pixels width and $1.2\times h_{Lower\text{-}Nose}$=30 pixels height as shown in Figure 2(c). The upper-left corner is denoted by point B5. The position of point B5 is also calculated by the following steps: (a) Let α_5=$0.5\times|1.2\times w_{Lower\text{-}Nose}-1.2\times w_{Upper\text{-}Nose}|$, and β_5=$h_{Upper\text{-}Nose}$; (b) The upper-left corner Point B5 ($x_{P_{B5}}$,$y_{P_{B5}}$) of Lower-Nose region can be located by Eq. (5). The process is illustrated in Figure 3(c).

$$x_{\mathrm{P_{B4}}} = x_{\mathrm{P_{37}}} - \alpha_4,\ y_{\mathrm{P_{B4}}} = y_{\mathrm{P_{29}}} - \beta_4 \tag{4}$$

$$x_{\mathrm{P_{B5}}} = x_{\mathrm{P_{B4}}} - \alpha_5,\ y_{\mathrm{P_{B5}}} = y_{\mathrm{P_{B4}}} + \beta_5 \tag{5}$$

4. The Left-Cheek region is defined as a rectangle of $1.0\times w_{Left\text{-}Cheek}$=30 pixels width and $1.2\times h_{Left\text{-}Cheek}$=60 pixels height. Its upper-left corner is denoted as point B6, as shown in Figure 2(c). The position of point B6 is calculated by the following steps: (a) Point C6 is the intersection of the horizontal line through point 1 and the vertical line through point 2; (b) The distance $\overline{P_1P_5}$ between point 1 and point 5 along the y-axis is calculated; (c) Let α_6=0, and β_6=$0.5\times|\overline{P_1P_5}-1.2\times h_{Left\text{-}Cheek}|$; (d) The upper-left corner B6 ($x_{P_{B6}}$,$y_{P_{B6}}$) is located by Eq. (6). Similarly, the position of point B7 can be calculated by Eq. (7) for the Right-Cheek rectangle region. And let $w_{Right\text{-}Cheek}=w_{Left\text{-}Cheek}$, $h_{Right\text{-}Cheek}=h_{Left\text{-}Cheek}$,$\alpha_7$=0 and β_7=$0.5\times|\overline{P_9P_{12}}-1.2\times h_{Right\text{-}Cheek}|$. The process is illustrated in Figure 3(d).

$$x_{\mathrm{P_{B6}}} = x_{\mathrm{P}_2} - \alpha_6,\ y_{\mathrm{P_{B6}}} = y_{\mathrm{P}_1} - \beta_6 \tag{6}$$

$$x_{\mathrm{P_{B7}}} = x_{\mathrm{P}_{12}} + \alpha_7,\ y_{\mathrm{P_{B7}}} = y_{\mathrm{P}_{13}} - \beta_7 \tag{7}$$

5. Finally, the Mouth region is defined as a rectangle region with $1.2\times w_{Mouth}$=48 pixels width and $3\times h_{Mouth}$=51 pixels height. The upper-left corner is denoted as point B8 as shown in Figure 2(c).The position of point B8 can be calculated as follows: (a) Point C8 is defined as the intersection of the horizontal line through point 50 and the vertical line through point 48; (b) $\overline{P_{48}P_{54}}$ between point 48 and point 54 along the x-axis and $\overline{P_{50}P_{57}}$ between point 50 and point 57 along the y-axis are calculated; (c) Let α_8 =$0.5\times|\overline{P_{48}P_{54}}-1.2\times w_{Mouth}|$, and β_8 =$0.5\times|\overline{P_{50}P_{57}}-1.2\times h_{Mouth}|$; (d) The upper-left corner Point B8 ($x_{P_{B8}}$,$y_{P_{B8}}$) is located by Eq. (8). The process can be seen from Figure 3(e).

$$x_{\mathrm{P_{B8}}} = x_{\mathrm{P}_{48}} - \alpha_8,\ y_{\mathrm{P_{B8}}} = y_{\mathrm{P}_{50}} - \beta_8 \tag{8}$$

2.4. Extraction of the movement feature

The LBP operator, which is proposed for texture analysis by Ojala et al. [19], has been proven to be robust against illumination changes [26]. It is also commonly used for recognition of facial expression [27]. Operator of $LBP_{8,2}^{u2}$ is selected to extract features of the eight regions in this paper. As a result, each image is presented by the LBP histograms with the length of 472 (59×8) as shown in Figure 4.

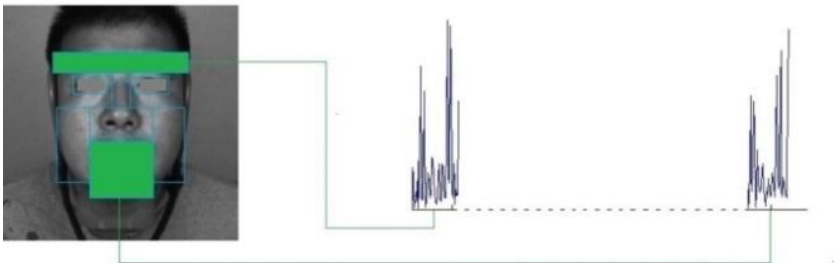

Fig. 4. Feature vector of an image built by concatenating feature histograms from each region of the eight regions.

3. Results and discussion

In this section, the proposed ASMLBP method is evaluated on the collected facial paralysis database which contains 570 (57×5×2) images of 57 patients (31 females and 26 males) with five facial movements. There are two images per patient for each of five key facial movements (raising eyebrows, closing eyes, screwing up nose, plumping cheek and opening mouth). Moreover, the ASMLBP is also tested on the JAFFE database for recognizing the patterns of facial movement. The JAFFE database contains 213 images of seven facial expressions posed by 10 Japanese female models, including one neutral expression and six facial expressions. The leave-one-out cross-validation strategy is used for estimating the performance of recognition accuracy.

A previously successful technique for facial expression classification is SVM [27] and SVM has a number of applications in the biomedical field [28,29]. Therefore, the experiment compares the classification performance of the proposed ASMLBP descriptors with five other famous facial features using SVM. The Local Phase Quantization (LPQ) operator was originally presented in [30], and has been combined with LBP for texture classification to achieve better performance. In experiments, the LBP and the LBP+LPQ features are extracted as full face descriptors. The face is also divided into 42(6×7) sub-blocks for feature extraction [27], and the LBP and the LBP+LPQ features are used to represent facial characteristics. Moreover, the Fixed-LBP feature is extracted from fixed positions of eight regions (Eyebrow, Left-Eye, Right-Eye, Upper-Nose, Lower-Nose, Left-Cheek, Right-Cheek and Mouth).

3.1. Result on facially paralyzed patient data

Table 1 shows the recognition rates of LBP, LBP+LPQ, LBP_{6*7}, $LBP+LPQ_{6*7}$, Fixed-LBP and ASMLBP (ASM+LBP) with SVM. It can be seen from Table 1 that the recognition rates of the method proposed in this paper are higher than other methods with various kernel functions of SVM. Especially with sigmoid, the result of the method in this paper is almost 3 times higher than the lowest one. Moreover, the proposed method has the highest recognition rate, which can reach 96.2963%. As for ASMLBP, when different kernel functions of SVM are used, the lowest recognition rate could also reach 93.9571%. The proposed method can achieve high robustness and accuracy on the faces of facially paralyzed patients.

Table 1

Comparison among different methods on the facial paralysis database

	Recognition Rate (%)				
	Linear	Polynomial(d=2)	Polynomial(d=3)	RBF	sigmoid
LBP	57.5049	42.1053	60.2339	66.6667	40.9357
LBP+LPQ	61.5984	43.8596	57.1150	72.5146	62.3782
LBP_{6*7}	92.5926	88.3041	80.1170	24.1715	30.6043
$LBP+LPQ_{6*7}$	92.0078	88.3041	75.4386	24.1715	35.8674
Fixed-LBP	95.1267	93.1774	92.0078	94.2963	92.0078
ASMLBP	**96.2963**	**95.9064**	**95.9064**	**95.9064**	**93.9571**

3.2. Result on JAFFE data

In the previous section, it can be seen that the proposed method obtains higher recognition rate on the collected facial paralysis database. In order to examine the generality of the proposed method, experiments are carried out on the publicly available JAFFE database for recognition of the facial expression. The method aims to automatically recognize the patterns of facial movement. The same facial movement pattern could occur in different facial expressions. For example, people open their mouth when happy or surprised. Therefore suitable images are selected based on the facial movement patterns, such as raising eyebrows, screwing up nose, plumping cheek and opening mouth. The results of recognition rates on the JAFFE database with SVM are shown in Table 2.

From Table 2, it can be observed that the proposed method can obtain a better recognition rate than others with linear, polynomial and sigmoid SVM. Meanwhile, with the linear kernel function, the proposed method can obtain the highest recognition rate of 93.3333%. This implies that the method proposed in this paper can also gain better performance on the normal human faces.

4. Conclusion

In this paper, a new method was presented to automatically recognize the patterns of facial movement from facially paralyzed patients. It can meet the requirement of the system that can evaluate the degree of facial paralysis automatically. In the proposed method, the ASMs were rained firstly by using facial paralysis images. Then, the trained model was used to locate the 68 key points on the face of a new patient. Next, the face was divided into eight regions based on the key points that were located by using ASMs. Fourthly, the LBP was utilized to extract descriptors from eight local regions and concatenate feature histograms from each of eight regions into a feature vector. Finally, SVMs with linear, Polynomial, RBF and sigmoid kernel functions were used to evaluate the performance of the proposed method. Experiments showed that the proposed method is accurate and robust on the collected facial paralysis database as well as the JAFFE database.

Future work will introduce the feature selection technique [31] to improve the performance of the classifier, and extend the proposed method for recognizing grimace or asymmetric facial movements of normal people. Moreover, extensive research will be carried out to evaluate the degree of facial paralysis based on the proposed method.

Table 2

Comparison among different methods on the JAFFE database

	Recognition Rate (%)				
	Linear	Polynomial (d=2)	Polynomial (d=3)	RBF	sigmoid
LBP	66.6667	36.6667	36.6667	**66.6667**	56.6667
LBP+LPQ	73.3333	56.6667	50.0000	36.6667	43.3333
LBP_{6*7}	83.3333	56.6667	50.0000	36.6667	63.3333
$LBP+LPQ_{6*7}$	83.3333	56.6667	50.0000	36.6667	63.3333
Fixed-LBP	90.0000	63.3333	56.6667	36.6667	43.3333
ASMLBP	**93.3333**	**63.3333**	**56.6667**	36.6667	**63.3333**

Acknowledgement

This work is supported by the National Natural Science Foundation of China (No. 61271405), Ph.D. Program Foundation of Ministry of Education of China (20120132110018), China Postdoctoral Science Foundation (No. 2014M551962) and Fundamental Research Funds for the Central Universities (No. 201413020).

References

[1] J.Y. Dong, Y. Lin and L.A. Liu, An approach to evaluation of degree of facial paralysis based on image processing and pattern recognition, Journal of Information Systems **5** (2008), 639–646.
[2] J.Y. Dong, L. Ma, Q. Li, S. Wang, L.A. Liu, Y. Lin and M. Jian, An approach for quantitative evaluation of the degree of facial paralysis based on salient point detection, International Symposium on Intelligent Information Technology Application Workshops**,** 2008, 483–486.
[3] K. Anguraj and S. Padma, Analysis of facial paralysis disease using image processing technique, International Journal of Computer Applications **54** (2012), 1–4.
[4] J.R. Delannoy and T.E. Ward, A preliminary investigation into the use of machine vision techniques for automating facial paralysis rehabilitation therapy, In Signals and Systems Conference, 2010, 228–232.
[5] K. Anguraj, R. Kandiban and K.S. Jayakumar, Facial paralysis diseases level detection using CEM algorithm for clinical applications, European Journal of Scientific Research **77** (2012), 543–548.
[6] M. Isono, K. Murata, H. Tanaka, M. Minoyama and H. Azuma, Computerized analysis of facial motions-objective evaluation of facial palsy, Nihon Jibiinkoka Gakkai Kaiho **97** (1994), 393–400.
[7] S. He, J.J. Soraghan, B.F. O'Reilly and D. Xing, Quantitative analysis of facial paralysis using local binary patterns in biomedical videos, IEEE Transactions on Biomedical Engineering **56** (2009), 1864–1870.
[8] S. He, J.J. Soraghan and B.F. O'Reilly, Biomedical image sequence analysis with application to automatic quantitative assessment of facial paralysis, Journal on Image and Video Processing **2007** (2007), 81282-1–81282-11.
[9] S. McGrenary, B.F. O'Reilly and J.J. Soraghan, Objective grading of facial paralysis using artificial intelligence analysis of video data, Proceedings of the 18th IEEE Symposium on Computer-Based Medical Systems, IEEE Computer Society, 2005, 587–592.
[10] P.N. Belhumeur, J.P. Hespanha and D. Kriegman, Eigenfaces vs. fisherfaces: Recognition using class specific linear projection, IEEE Transactions on Pattern Analysis and Machine Intelligence **19** (1997), 711–720.
[11] Z. Zhang, M. Lyons, M. Schuster and S. Akamatsu, Comparison between geometry-based and gabor-wavelets-based facial expression recognition using multi-layer perceptron, Proceedings of Third IEEE International Conference on Automatic Face and Gesture Recognition, 1998, 454–459.
[12] G. Zhao and M. Pietikainen, Dynamic texture recognition using local binary patterns with an application to facial expressions, IEEE Transactions on Pattern Analysis and Machine Intelligence **29** (2007), 915–928.
[13] W. Gu, C. Xiang, Y.V. Venkatesh, D. Huang and H. Lin, Facial expression recognition using radial encoding of local Gabor features and classifier synthesis, Pattern Recognition **45** (2012), 80–91.
[14] M.S. Bartlett, G. Littlewort, M. Frank, C. Lainscsek, I. Fasel and J. Movellan, Recognizing facial expression: Machine learning and application to spontaneous behavior, IEEE Computer Society Conference on Computer Vision and Pattern Recognition **2** (2005), 568–573.
[15] Y.L. Tian, T. Kanade and J.F. Cohn, Recognizing action units for facial expression analysis, IEEE Transactions on Pattern Analysis and Machine Intelligence **23** (2001), 97–115.
[16] J.J.J. Lien, Automatic recognition of facial expressions using hidden MARKOV models and estimation of expression intensity, Ph.D. Dissertation, Washington University, 1998.
[17] T. Otsuka and J. Ohya, Spotting segments displaying facial expression from image sequences using HMM, Proceedings of Third IEEE International Conference on Automatic Face and Gesture Recognition, 1998, 442–447.
[18] T.F. Cootes, C.J. Taylor, D.H. Cooper and J. Graham, Active shape models-their training and application, Computer Vision and Image Understanding **61** (1995), 38–59.
[19] T. Ojala, M. Pietikäinen and T. Maenpaa, Multi-resolution gray-scale and rotation invariant texture classification with local binary patterns, IEEE Transactions on Pattern Analysis and Machine Intelligence **24** (2002), 971–987.
[20] M.J. Lyons, S. Akamatsu, M. Kamachi and J. Gyoba, The Japanese Female Facial Expression (JAFFE) database, http://www.kasrl.org/jaffe.html, Feb. 27, 2010.

[21] Y. Liu, K.L. Schmidt, J.F. Cohn and S. Mitra, Facial asymmetry quantification for expression invariant human identification, Computer Vision and Image Understanding **91** (2003), 138–159.
[22] A.L. Yuille, P.W. Hallinan and D.S. Cohen, Feature extraction from faces using deformable templates, International Journal of Computer Vision **8** (1992), 99–111.
[23] M. Kass, A. Witkin and D. Terzopoulos, Snakes: Active contour models. International journal of computer vision **1** (1988), 321–331.
[24] P. Felzenszwalb, D. McAllester and D. Ramanan, A discriminatively trained, multiscale, deformable part model, IEEE Conference on Computer Vision and Pattern Recognition, 2008, 1–8.
[25] K.W. Wan, K.M. Lam and K.C. Ng, An accurate active shape model for facial feature extraction, Pattern Recognition Letters **26** (2005), 2409–2423.
[26] M. Heikkilä, M. Pietikäinen and C. Schmid, Description of interest regions with local binary patterns, Pattern Recognition **42** (2009), 425–436.
[27] C. Shan, S. Gong and P.W. McOwan, Facial expression recognition based on local binary patterns: A comprehensive study, Image and Vision Computing **27** (2009), 803–816.
[28] X. Jie, R. Cao and L. Li, Emotion recognition based on the sample entropy of EEG, Bio-Medical Materials and Eengineering **24** (2014), 1185–1192.
[29] A. Subasi, Classification of EMG signals using PSO optimized SVM for diagnosis of neuromuscular disorders, Computers in Biology and Medicine **43** (2013), 576–586.
[30] V. Ojansivu and J. Heikkilä, Blur insensitive texture classification using local phase quantization, Proceedings of the 3rd International Conference on Image and Signal Processing (2008), 236–243.
[31] X. Sun, Y. Liu, J. Li, J. Zhu, H. Chen and X. Liu, Feature evaluation and selection with cooperative game theory, Pattern Recognition **45** (2012), 2992–3002.